De novo Peptides Modeling the Binding Sites of [4Fe-4S] Clusters in Photosystem I

6 AUTHORS, INCLUDING:

Mikhail L Antonkine
Bavarian Research Alliance

31 PUBLICATIONS **475** CITATIONS

Boris Epel
University of Chicago

69 PUBLICATIONS **1,036** CITATIONS

De novo Peptides Modeling the Binding Sites of [4Fe-4S] Clusters in Photosystem I

Mikhail L. Antonkine[1,2], Christoph Breitenstein[1], Boris Epel[1], Eckhard Bill[1], Wolfgang Gärtner[1], and Wolfgang Lubitz[1]

Abstract Photosystem I (PS I) converts the energy of light into chemical energy. The terminal electron transfer cofactors in PS I are three iron-sulfur clusters named F_X, F_A and F_B. The PsaC subunit of PS I harbors binding sites of the [4Fe-4S] clusters F_A and F_B. We modeled them by preparing two peptides (maquettes), sixteen amino acids each, using F_{moc} solid state peptide synthesis. These model peptides incorporate the consensus iron-sulfur binding motif along with amino acids from the immediate environment of the respective iron-sulfur cluster. The [4Fe-4S] clusters were successfully incorporated into these model peptides, as shown by their optical absorbance, EPR and Mössbauer spectra. The oxidation-reduction potential of the iron-sulfur clusters in the model peptides is close to that of F_A and F_B in PsaC at room temperature and is considerably lower than that observed for other [4Fe-4S] model systems described earlier.

[1] Max-Planck-Institut für Bioanorganische Chemie, Mülheim an der Ruhr, Germany
[2] Fachbereich Physik, Institut für Experimentalphysik, Freie Universität Berlin, Germany

Introduction

Three low-potential [4Fe-4S] clusters are part of the electron transfer chain of photosystem I (PS I), usually they are referred as F_X, F_A and F_B (reviewed in Vassiliev et al. 2001). The Iron-sulfur clusters F_A and F_B are bound to the PsaC subunit of PS I, which is located on the stromal side of the thylakoid membrane. PsaC has sequence similarity to bacterial dicluster ferredoxins.

Owing to their biological significance, several attempts to synthesize model compounds (reviewed in Rao and Holm 2004) and peptide-ligated [4Fe-4S] were made (Gibney et al. 1996; Coldren et al. 1997; Scott and Biggins 1997; Mulholland et al. 1998, 1999). For the latter, two main approaches were explored: the first relies on designing synthetic peptides containing an iron-sulfur binding site (Gibney et al. 1996; Mulholland et al. 1998, 1999); the second relies on introduction of the iron-sulfur cluster-binding site into a natural or synthetic protein that previously was incapable

of binding iron-sulfur clusters (Coldren et al. 1997; Scott and Biggins 1997).

This work has the following goals: first, to model the binding sites of the [4Fe-4S] clusters F_A and F_B of PS I; second, to investigate the biochemical and biophysical properties of the model systems by spectroscopic techniques and to compare them to the [4Fe-4S] clusters F_A and F_B bound to the PS I subunit PsaC.

Materials and methods

Peptide synthesis. Peptide synthesis was performed on an Advanced Chemtec 348 Ω synthesizer. The overall yield after purification (>99%) was 17% for both peptides. Purity was proven by analytical HPLC and MALDI-TOF-MS (Matrix Assisted Laser Desorption Ionisation – Time-of-Flight-Mass Spectrometry) for apo-F_A (found 1850.5, calc. 1852.8) and apo-F_B (found 1845.6, calc. 1845.7). The [4Fe-4S] clusters were inserted into the apo-peptide by a procedure similar to that originally described (Lovenberg et al. 1963).

Redox titration. The redox potential was determined in a thin-layer three-electrode cell inside a glove box. A reference Ag/AgCl electrode was used and working and counter electrodes were made from glassy carbon. The potential of the reference electrode was determined by measuring the mediator methyl viologen. The use of redox mediators had no measurable effect on the redox potential.

EPR experiments. Continuous wave EPR samples were measured on a Bruker E500 spectrometer operating at X-band. The temperature was controlled by an Oxford ESR continuous flow cryostat model 910 combined with an Oxford ITC 503 intelligent temperature controller. Sample was reduced by addition of sodium dithionite at pH=10.

Results

Design of model peptides

The sequence similarity between PsaC and bacterial dicluster ferredoxins is restricted to the two [4Fe-4S] cluster binding motifs C(I)xxC(II)xxC(III)xxxC(IV)P and C(I')xxC(II')xxC(III')xxxC(IV')P.

Cysteines I, II, III and IV' ligate the first iron-sulfur cluster (F_B) and cysteines I', II', III' and IV ligate the second iron-sulfur cluster (F_A). In our design approach these two ligation schemes are separated into two distinct peptides. The obvious point to dissociate the two binding sites is between cysteine IV and cysteine I'. In a second step the fourth ligand for each binding site needs to be relocated to get into close vicinity to the first three cysteines. This can be achieved by introducing a short loop consisting of the residues KPE, where Pro is supposed to initiate the loop formation and the residues lysine and glutamate form a salt bridge to stabilize the preformed turn. Except for the designed loop region, the native amino acid sequence of PsaC has been used, i.e. Tyr 7 to Cys 16 for the sequence TEDCVGCKRCKPECPW (apo-F_B peptide); Thr 44 to Cys 53 for the sequence YDTCIGCTQCKPECPW (apo-F_A peptide). These sequences are especially interesting since they show major differences in amino acid composition in the consensus binding motif with respect to previously investigated model peptides that bind [4Fe-4S] clusters.

Characterization of model peptides. After synthesis and insertion of iron-sulfur clusters into apo peptides (see methods) both holo-F_A and holo-F_B peptides show a broad absorption in the visible range with a maximum around 400 nm, which is reduced by approximately 50% of its initial intensity upon reduction of the sample with sodium dithionite (Fig. 1A). In summary, the UV/Vis spectra of the holo-F_A and holo-F_B peptides in the oxidized and reduced states are typical for protein/peptide-bound iron-sulfur clusters.

We used CW EPR spectroscopy to probe the identity of the iron-sulfur clusters bound to the holo-F_A and holo-F_B peptides. In the reduced state the holo-F_A peptide has a rhombic EPR spectrum with g-values 2.04 (g_x), 1.93 (g_y), 1.90 (g_z) (Fig. 1B), while the holo-F_B peptide has a rhombic EPR spectrum with g-values 2.05 (g_x), 1.93 (g_y), and 1.92 (g_z). EPR signals of the [4Fe-4S] clusters bound to the holo-F_A and holo-F_B peptides can be observed only at temperatures below 40 K and they show a strong temperature dependence. The g-values and relaxation properties, i.e. microwave power and temperature dependence, of holo-F_A
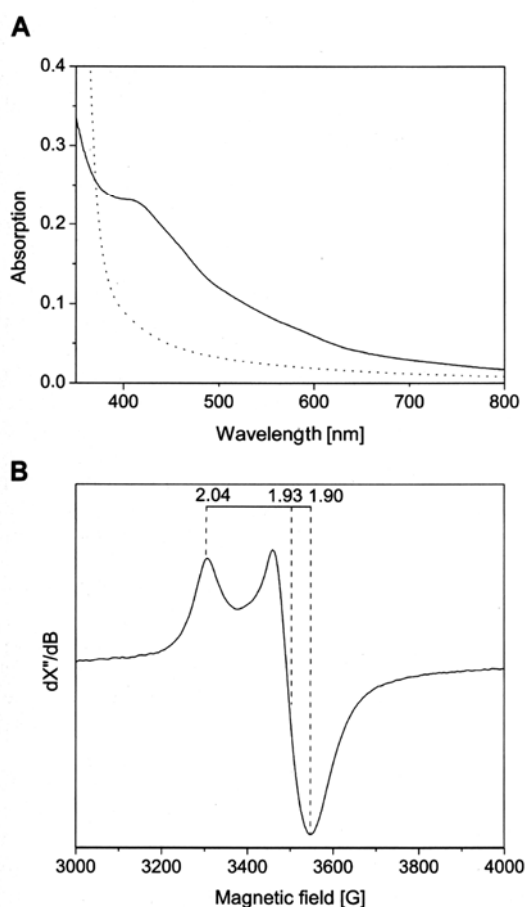
A

B

Fig. 1 A. UV-visible spectra of the holo-F_A peptide in the oxidised (solid line) and reduced (dashed line) state. **B.** EPR spectra of the reduced holo-F_A peptide. EPR conditions: temperature 15 K, microwave frequency 9.436 GHz, microwave power 10 mW, modulation frequency 100 kHz, modulation amplitude 10 G

and holo-F_B peptides are typical of reduced [4Fe-4S] proteins. Similar EPR spectra were observed earlier for mono cluster ferredoxins, model peptides (Gibney et al. 1996; Mulholland et al. 1998, 1999) and in PsaC (C13G C33S and C50G C33S mutants), where one of the iron-sulfur clusters is not detectable in the $g = 2$ region of the EPR spectrum (Antonkine et al. 2007). Binding of the [4Fe-4S] cluster to apo-F_A and apo-F_B peptides is verified by the Mössbauer spectra of the holo-F_A and holo-F_B peptides in both oxidized and reduced states (data not shown).

Oxidation-reduction potential of the holo-F_A and holo-F_B peptides

Reduction of the sample by sodium dithionite was followed by optical spectroscopy, additionally at several potentials EPR samples were taken to independently control the reduction of [4Fe-4S]. The titrations were stopped when excess of the dithionite was detectable by optical spectroscopy. This corresponds to a complete reduction of the sample. The redox titration resulted in redox potentials of −490 ± 30 mV and −475 ± 30 mV (all potentials vs. SHE) for holo-F_A and holo-F_B peptides respectively.

Discussion

We successfully modelled the [4Fe-4S] clusters F_A and F_B of the PsaC subunits of PS I. By several techniques we have proven that low-potential [4Fe-4S] clusters are formed with both model peptides.

Fully reduced, unbound wild-type PsaC shows an interaction spectrum due to magnetic coupling between the two closely-spaced $S = 1/2$ [4Fe-4S]$^{1+}$ clusters. The EPR spectra of unmodified cluster F_A of PsaC can be observed in the C13G C33S variant of the protein ($g_x = 2.04$, $g_y = 1.93$ and $g_z = 1.90$) and of F_B in the C50G C33S variant ($g_x = 2.04$, $g_y = 1.93$ and $g_z = 1.89$) (Antonkine et al. 2007). These values are identical to those obtained for the holo-F_A and only slightly different for the holo-F_B, with $g_z = 1.92$.

Despite the variation of amino acid composition most of the maquettes investigated in previous studies have a redox potential of about −350 mV (Gibney et al. 1996; Mulholland et al. 1998, 1999). Scott and Biggins (1997) incorporated a binding motif of the [4Fe-4S] cluster F_X into a 4-α-helix bundle. This model exhibits the lowest reduction potential found for the [4Fe-4S] cluster bound to peptide maquette up to date (−420 mV). Midpoint reduction potentials of F_A and F_B in fully assembled PS I were measured at cryogenic temperature by redox titration with EPR detection and found to be −540 and −590 mV respectively (Evans and Heathcote 1980). However, by titration of PS I with optical detection of charge recombination between

the iron-sulfur clusters and P700$^+$ at room temperature potentials of −465 and −440 mV were found for F_A and F_B, respectively (Jordan et al. 1998). The latter potentials are closer to typical midpoint redox potentials found for [4Fe-4S] clusters in bacterial ferredoxins. They are also within the error range of the potentials that were determined for the peptides modeling the binding sites of [4Fe-4S] clusters F_A and F_B in this work.

References

Antonkine ML, Maes EM, Czernuszewicz RS, Breitenstein C, Bill E, Falzone CJ, Balasubramanian R, Lubner C, Bryant DA, Golbeck JH (2007) Chemical rescue of a site-modified ligand to a [4Fe-4S] cluster in PsaC, a bacterial-like dicluster ferredoxin bound to photosystem I. Biochim Biophys Acta 1767:712–724.

Coldren CD, Hellinga HW, Caradonna JP (1997) The rational design and construction of a cuboidal iron-sulfur protein. Proc Natl Acad Sci USA 94:6635–6640.

Evans MCW, Heathcote P (1980) Effects of glycerol on the redox properties of the electron acceptor complex in spinach photosystem I particles. Biochim Biophys Acta 590:89–96.

Gibney BR, Mulholland SE, Rabanal F, Dutton PL (1996) Ferredoxin and ferredoxin-heme maquettes. Proc Natl Acad Sci USA 93:15041–15046.

Jordan R, Nessau U, Schlodder E (1998) Charge recombination between the reduced iron-sulfur clusters and P700$^+$. In: Garab G (ed) Photosynthesis: Mechanisms and Effects, Vol. 2. Kluwer, Dordrecht, The Netherlands. pp. 663–666.

Lovenberg W, Rabinowitz JC, Buchanan BB (1963) Studies on chemical nature of Clostridial ferredoxin. J Biol Chem 238:3899–3913.

Mulholland SE, Gibney BR, Rabanal F, Dutton PL (1998) Characterization of the fundamental protein ligand requirements of [4Fe-4S](2 + /+) clusters with sixteen amino acid maquettes. J Am Chem Soc 120:10296–10302.

Mulholland SE, Gibney BR, Rabanal F, Dutton PL (1999) Determination of nonligand amino acids critical to 4Fe-4S (2+/+) assembly in ferredoxin maquettes. Biochemistry 38:10442–10448.

Rao PV, Holm RH (2004) Synthetic analogues of the active sites of iron-sulfur proteins. Chem Rev 104:527–559.

Scott MP, Biggins J (1997) Introduction of a [4Fe-4S (S-cys)4](+1, + 2) iron-sulfur center into a four-α helix protein using design parameters from the domain of the F_X cluster in the Photosystem I reaction center. Protein Sci 6:340–346.

Vassiliev IR, Antonkine ML, Golbeck JH (2001) Iron-sulfur clusters in type I reaction centers. Biochim Biophys Acta 1507:139–160.